Broadband Monolithic Constrained Lens Design

by

Leonard Thomas Hall

B.E. (Electrical & Electronic, with Honours),
The University of Adelaide, Australia, 2000

Thesis submitted for the degree of

Doctor of Philosophy

in

School of Electrical and Electronic Engineering,
Faculty of Engineering, Computer and Mathematical Sciences
The University of Adelaide, Australia

August, 2009

Chapter 1

Introduction and Motivation

THE growing complexity of radar and communications systems has created a need for antennas capable of forming multiple simultaneous beams. At the heart of these antennas is a beam-forming network capable of generating multiple, independent, highly directional beam patterns, using a single linear antenna array. While many techniques exist, this thesis focuses on the beam-forming network known as the Rotman lens. Developed in 1963 by Rotman and Turner, the Rotman lens is a passive structure capable of driving arrays containing hundreds of broadband elements.

While the Rotman lens has been implemented using a number of different transmission media, few are as compact and inexpensive as microstrip. Using standard monolithic manufacturing techniques, microstrip lenses can include active elements, such as low noise amplifiers and power amplifiers, and passive elements such as power dividers and antennas. This combination is particularly attractive for systems operating at millimetre wavelengths.

This thesis examines the Rotman lens to determine its potential as a broadband beam-forming network.

1.1 Thesis Overview

One of the key ideas developed in this thesis is that a Rotman lens, or any constrained lens, is simply a number of transmission lines connecting antenna elements. Beam ports are treated as closely spaced antenna elements, and antenna ports as elements of a nonlinear antenna array. Although the beam ports and antenna ports of a modern Rotman lens are hardly recognisable as antenna elements, their treatment as such is shown to be at the heart of a successful lens design. This approach is used to address the challenges of port impedance mismatch, port mutual coupling, and unwanted reflections from the lens sidewall. This thesis explores these problems and provides a methodology for addressing these challenges.

This chapter opens with an introduction and motivation, followed by a summary of the key contributions presented in this thesis. Chapter 2 begins with a brief history of electromagnetism describing the work of Maxwell and Hertz. A short history of antenna element and antenna array development is presented introducing a more detailed summary of antenna theory. This is extended to describe the behaviour of arrays of antenna elements and introduces some of the popular methods of feeding these arrays. Chapter 2 concludes with a description of the first Rotman lens and explains why this simple structure has generated so much interest in the literature.

Chapter 3 presents transmission line theory and multi-port network parameters, which are engineering tools needed to develop microwave lenses and connecting circuits. The *Telegraphers' Equations* are used to derive transmission line parameters and introduce reflection coefficient and impedance transformation. Multi-port networks are introduced using the impedance and admittance matrices. These concepts are developed into S-parameters and generalised S-parameters. The alternative travelling wave formulations of pseudo-wave and power-wave scattering parameters are introduced and why they are needed for multi-port matching is explained. A number of impedance matching techniques are then described and the chapter concludes with a short comparison of their relative merits.

Chapter 4 describes the Rotman lens in detail and explores the history of Rotman lens development. The Rotman parameters are defined and their effect on lens shape is presented. A brief summary of the significant contributions in lens analysis is included, and latest approaches to lens design are discussed. Chapter 4 finishes by describing the historical development of Rotman lens implementation and summarises the significant advances in this area.

Chapter 5 closely examines the properties of the Rotman equations and their application to linear antenna array feed network design. The Rotman equations are re-written in a form more appropriate for this task and an improved method of characterising the lens aberrations is described. This method is used to comment on optimal focal arc geometry and the effectiveness of approximations commonly used in the literature.

Chapter 6 presents the software tools used to conduct and analyse the experiments described in this thesis. This is followed by the methods used to gather measured data from the realised lens designs. A description of the numerous ways the performance of a constrained lens is measured, and how these measures are derived from simulated and experimental results is also provided.

Chapter 7 explores the key areas of constrained lens implementation. By treating lens ports as antenna elements in an array or in the presence of other elements, this chapter examines the effects of port geometry, spacing, and impedance in the broadband constrained lens application. This analysis defines clear limitations of constrained lens performance that have not been identified in the literature. The chapter continues by tackling the significant broadband, multi-port, matching problem. An effective matching solution is described and applied to single, multiple fixed phase, and multiple variable phase port matching. Finally, the techniques described within this thesis are applied to four lens designs.

The major conclusions and future directions of this work are summarised in Chapter 8.

1.2 Original Contributions

This thesis makes a number of significant contributions to the analysis, design and implementation of the Rotman lens and constrained lenses in general.

The Rotman equations define the lens geometry and aberrations in terms of the lens focal length rather than aperture size. This is not consistent with the role of a beam-forming network for a linear phased array. The renormalisation of the Rotman equations by the aperture size rather than the focal arc paves the way for a thorough analysis of the Rotman lenses in this role. Further, the accepted method of defining lens aberration performance measures the maximum deviation from the theoretical linear wavefront. This does not translate well to the beam-forming performance of the lens. An improved aberration measure is proposed and then used to examine the relationship between aberration performance and the five Rotman parameters Sec. 5.1 and 5.2.

The Rotman equations do not define the focal arc connecting the three focal points of the lens. Using numerical methods, the focal arc of the Rotman lens is optimised for a large range of parameter values. This analysis shows that the circular focal arc results in the lowest path length errors of any focal arc shape (Sec. 5.3).

The ports of the Rotman lens are analysed as antenna elements to clearly define the mechanisms that limit monolithic constrained lens performance. Significant insight has been gained by focusing on the performance of an individual port, both in isolation and in the presence of other ports. This provides a clear understanding of how port geometry and substrate choice is used to improve lens aberrations and simplify the task of port matching. In addition, the coupling of energy to adjacent ports is a significant limiting factor of lens performance. By examining port coupling and impedance properties, fundamental monolithic constrained lens limitations are defined (Sec. 7.1).

Impedance matching of linear phased antenna arrays and antenna ports of a Rotman lens are very similar problems. The lens matching problem is complicated further by the need to simultaneously match the beam and dummy ports. This is successfully addressed by applying an iterative impedance matching algorithm using the power-wave formulation of generalised S-parameters. This matching algorithm accounts for single port excitations, simultaneous fixed phase port excitations and multiple variable phase port excitations. This matching algorithm significantly improves the performance of broadband lenses and is also useful for matching closely spaced antenna arrays and multi-port networks (Sec. 7.3).

The critical issue of lens sidewall implementation is addressed using dummy ports terminated with microstrip loads. This motivated the design of two microstrip load designs. The first is a compact, narrow-band load, while the second is a larger broadband load (Sec. 7.4).

Finally the numerous methods and tools are combined to design and manufacture a number of constrained lenses. Two narrow-band Rotman lenses with an integrated linear antenna array are designed and characterised. To demonstrate the effectiveness of broadband port design and matching, a third Rotman lens design is presented. The performance and bandwidth of these lenses provide a benchmark from which state-of-the-art can be defined (Sec. 7.5).

Chapter 2

Background

TO fully appreciate the intricacies of constrained lens design, the fundamentals of antenna element and antenna array design should be clearly understood. This chapter presents a brief history of antennas and propagation followed by an introduction to antenna fundamentals. The principles of beam-forming using arrays of antenna elements is then presented, followed by a summary of the power dividing networks used to feed such arrays.

To understand the significance of the most popular of constrained lens architectures, the Rotman lens, it is necessary to provide a review of constrained lens development. The evolution of constrained lenses from dielectric lenses and reflector antennas is presented. The concept of the bootlace lens is explained, followed by descriptions of lens geometries suitable for driving both circular and linear antenna arrays.

2.1 Brief History of Antennas and Propagation

An antenna is the transitional structure between free-space and a guiding device for propagating electromagnetic energy (Balanis 1997). The guiding device could be any number of transmission line types. The transmission line ensures efficient energy transfer between the antenna and the rest of the system.

The first publications on the design of antenna elements and their application, to generating electromagnetic waves, is found through the work of science historians (Kraus 1985, Gordon 1985, Garratt 1995, Sengupta and Sarkar 2003). James Clerk Maxwell's radical concept of *displacement current* brought together the work of Hans C. Oersted (1777-1851), Carl F. Gauss (1777-1855), André-Marie Ampère (1775-1836), Michael Faraday (1791-1867), and others in the form of Maxwell's equations (Maxwell 1865, Maxwell 1873). Maxwell, pictured in Figure 2.1(a), showed that a planar electromagnetic wave travelling in free space does so at the velocity of light and the wave consists of both electric and magnetic components that lie in the plane perpendicular to the direction of propagation. These components are mutually orthogonal, and propagate together. Maxwell did not live to see his work confirmed by experiments performed by Hertz (1888), pictured in Figure 2.1(b).

Heinrich Rudolph Hertz, as professor at the Technical Institute in Karlsruhe, assembled the first complete radio system in 1886. The system consisted of an end-loaded half-wave dipole as the transmitting antenna and a resonant loop antenna as the receiver. When sparks were produced at a gap at the centre of the dipole, sparking also occurred at a gap in the nearby loop (Bryant 1988). During the next two years, Hertz extended his experiments demonstrating reflection, refraction and polarisation, showing that radio waves and light are the same phenomenon, differing only in their wave length and frequency. In his 1890 paper, Hertz expressed Maxwell's equations in component form and brought a new clarity to Maxwell's theory (Hertz 1890).

Hertz's equipment remained merely a laboratory experiment until Guglielmo Marconi showed that electromagnetic waves could be used to send messages (Friedel 1981, Friedel 1984). Marconi quickly incorporated tuning and larger antennas for longer wavelengths in attempts to transmit over ever increasing distances. In December 1901, he successfully received radio signals sent across the Atlantic and in doing so started a wireless revolution.

While World War I drove the development of wireless communications, World War II saw the maturity of radar and the emergence of many new forms of antenna, see Figure 2.2.

(a) James Clerk Maxwell (1831-1879)

(b) Heinrich Rudolph Hertz (1857-1894)

Fig. 2.1: Founders of radio. James Clerk Maxwell and Heinrich Rudolph Hertz are credited for the basis of electromagnetic theory today (Friedel 1981). Despite Maxwell's insight into electromagnetic propagation, there is no indication that he thought waves could be generated electrically, it was Hertz that demonstrated the first radio system in 1886.

Radar required high gain, directional antennas and ever increasing bandwidth. For the first time, antenna elements were constructed using long tapered conductors rather than the shorter resonant lengths demonstrated practical broadband antennas (Balanis 1997).

The two decades before 1940 contained much activity on array theory and experimentation. Some of the prominent researchers were G. H. Brown, E. Bruce, P. S. Carter, C. W. Hansell, A. W. Ladner, N. E. Lindenblad, A. A. Pistolkors, S. A. Schelkunoff, G. C. Southworth, E. J. Sterba, and T. Walmsley. During World War II, much array work was performed in Britain and the United States. Beam-forming and beam-steering attracted significant interest as a solution to creating large apertures without the mechanical problems associated with a large single element (Pistolkors 1929, Southworth 1930, Bruce 1931, Carter et al. 1931, Sterba 1931, Bruce and Beck 1935, Brown 1937, Schelkunoff 1943, Silver 1949). The complexity of feed networks for large arrays posed significant problems. Time delay and phase delay networks, such as the Blass and Butler matrices, achieved good results (Blass 1960, Butler and Lowe 1961). Comparatively low cost and reduced

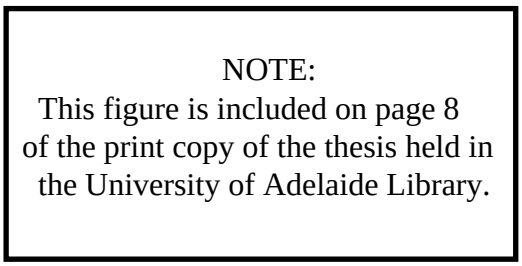

Figure 2.2: SCR-270 radar antenna array. The SCR-270-BA uses a 4 by 8 antenna element array of half wave dipoles, resonant at 104-112 MHz, with a beamwidth of 12 degrees. The SCR-270-BA is a pulsed radar with a peak power of 100 kW and was developed in 1938 and put into service in 1941. After Vieweger and White (2003).

complexity made lens solutions appealing (Kock 1946, Ruze 1950, Gent 1957, Rotman and Turner 1963). The first extensive coverage of phased arrays was the publication by Academic Press of the three-volume book *Microwave Scanning Antennas*, with volume 1 appearing in 1964, and volumes 2 and 3 in 1966 (Hansen 1964).

The early 1950's produced a small, lightweight, and conformal antenna element called the *patch antenna* (Deschamps and Sichak 1953, Gutton and Baissinot 1955, Munson 1974, Howell 1975, Pozar 1992). At millimetre-wavelengths the patch antenna combined with microstrip and stripline circuitry has made conformal, compact, high gain, steered beam antenna arrays practical.

2.2 Antenna and Linear Array Principles

An antenna radiates electromagnetic energy into free space from a transmitter, or conveys electromagnetic energy extracted from free space to a receiver. The following section provides the parameters that are used to describe antennas in these roles. These properties are divided into two categories; those describing the radiation characteristics and those describing the electrical characteristics of the antenna element. Finally these antenna properties are presented in the context of the *Friis transmission equation* and the *radar range equation*.

This section continues with the discussion of antenna elements combined in a linear array. Understanding antenna array principles is critical to understanding both the purpose, and the inner workings, of constrained lenses. Critical concepts of mutual coupling and mutual impedance are explained, along with the basic array theory of beam-forming and beam-steering.

2.2.1 The Antenna Element

The radiation characteristics are most commonly described in terms of the antenna radiation pattern. The radiation pattern is a mathematical function or graphical representation of the radiation properties of the antenna as a function of space coordinates. In most cases, the radiation pattern is determined in the far-field region and is represented as a function of the directional coordinates. Radiation properties including power flux density, radiation intensity, field strength, directivity, phase or polarisation (IEEE Standard 1993).

The *directivity* parameter measures the ability of the radiating structure to direct the electromagnetic energy in a preferred direction. An isotropic antenna is one that radiates equally in all directions. Although an isotropic antenna is impossible to implement, it is used as a conceptual reference from which we define directivity.

If single beam antenna has higher directivity, it radiates more effectively in one direction than in all others while an antenna with low directivity emits radiation in all directions. The directivity of an antenna is defined as the the ratio of the radiation intensity in a given direction from the antenna to the radiation intensity averaged over all directions. The average radiation intensity is equal to the total power radiated by the antenna divided by 4π. If the direction is not specified, the direction of maximum radiation intensity is

implied (IEEE Standard 1993). This is expressed by:

$$\begin{aligned} D &= \frac{U}{U_0}, \\ &= \frac{4\pi U}{P_{\text{rad}}}, \\ D_{\max} &= \frac{4\pi U_{\max}}{P_{\text{rad}}}, \end{aligned}$$

where

$$\begin{aligned} D &= \text{directivity (dimensionless)}, \\ U &= \text{radiation intensity (W/unit solid angle)}, \\ U_{\max} &= \text{maximum radiation intensity (W/unit solid angle)}, \\ U_0 &= \text{radiation intensity of isotropic source (W/unit solid angle)}, \\ P_{\text{rad}} &= \text{total radiated power (W)}. \end{aligned}$$

The parameters directivity and *gain* are similar concepts, however gain also includes the efficiency of the antenna. Gain is defined as the ratio of the radiation intensity, in a given direction, to the radiation intensity that would be obtained if the power accepted by the antenna were radiated isotropically. The radiation intensity corresponding to the isotropically radiated power is equal to the power accepted by the antenna divided by 4π. Gain does not include losses arising from impedance and polarisation mismatches (IEEE Standard 1993). This is expressed by:

$$\begin{aligned} G &= \frac{4\pi U}{P_{\text{in}}}, \\ G(\theta,\phi) &= eD(\theta,\phi), \\ G_{\max} &= \frac{4\pi U_{\max}}{P_{\text{in}}}, \\ G_{\max} &= eD_{\max}, \end{aligned}$$

where

$$\begin{aligned} e &= \text{antenna radiation efficiency (dimensionless)}, \\ &= \frac{P_{\text{rad}}}{P_{\text{in}}}, \\ P_{\text{in}} &= \text{total accepted power (W)}. \end{aligned}$$

The *effective area* in a given direction is defined as the ratio of the available power at the terminals of a receiving antenna to the power flux density of a plane wave incident on the antenna from that direction, the wave being polarisation matched to the antenna.

If the direction is not specified, the direction of maximum radiation intensity is implied (IEEE Standard 1983). The effective area can be written as:

$$A_e = \frac{P_T}{W_i},$$

where

$$\begin{aligned} A_e &= \text{effective area or aperture } (\text{m}^2), \\ P_T &= \text{power delivered to the load (W)}, \\ W_i &= \text{power density of incident wave } (\text{W/m}^2). \end{aligned}$$

The maximum effective area, A_{em}, is related to the maximum directivity, D_0, by:

$$A_{\text{em}} = \frac{\lambda^2}{4\pi} D_0.$$

This equation suggests that to achieve high directivity in a chosen direction the area of the antenna must be large when projected onto the plane perpendicular to that direction.

The *half-power beamwidth* is the angle between the two directions in which the radiation intensity is one-half the maximum value, in a radiation pattern cut containing the direction of the maximum of a lobe (IEEE Standard 1993).

The *polarisation* of an antenna in a given direction is the same as the polarisation of the radiated wave in that direction. This is defined as that property of an electromagnetic wave describing the time varying direction and relative magnitude of the electric-field vector; specifically, the figure traced as a function of time by the extremity of the vector at a fixed location in space, and the sense in which it is traced, as observed along the direction of propagation (IEEE Standard 1983, Balanis 1997).

In the most general case, the figure traced by the E-field vector is elliptical. Two special cases are linear polarisation where the ellipse collapses into a line or circular polarisation where the ellipse becomes circular. Linear polarisation is produced when the x and y components of the E-field are in phase, producing a varying electric field in a particular orientation. Linear polarisations are classified based on the angular orientation of the E-field. Circular polarisation is produced when the x and y components are 90° out of phase, producing an E-field of constant magnitude that rotates about the direction of propagation. Circular polarisations are classified based on the direction of rotation about the propagation vector.

Polarisation is largely predictable from antenna construction, however the polarisation of side lobes can be quite different from that of the main propagation lobe. In practice

it is important that the polarisation of transmit and receive antennas be matched. If mismatch exists, the received signal strength is reduced.

Electrical Characteristics

The electrical characteristics of the antenna, connected to terminals a and b in Figure 2.3(a), are described by the antenna *Input Impedance*. The input impedance is defined as the impedance presented by an antenna at its terminals (IEEE Standard 1993). The impedance of the antenna is expressed as:

$$Z_A = R_A + jX_A, \tag{2.1}$$

where

$$\begin{aligned} Z_A &= \text{antenna impedance (ohms)}, \\ R_A &= \text{antenna resistance (ohms)}, \\ X_A &= \text{antenna reactance (ohms)}. \end{aligned}$$

The resistive component of the antenna impedance is divided into two parts, the *radiation resistance* and the *loss resistance*:

$$R_A = R_r + R_L,$$

where

$$\begin{aligned} R_r &= \text{radiation resistance (ohms)}, \\ R_L &= \text{loss resistance (ohms)}. \end{aligned}$$

Energy absorbed to the radiation resistance is converted to electromagnetic energy and radiated into free space. The energy absorbed by the loss resistance is converted to heat within the antenna. These definitions lead to a simple definition of *Antenna Radiation Efficiency*, the ratio of the total power radiated by an antenna to the net power accepted by the antenna from the connected transmitter (IEEE Standard 1993). This is expressed by:

$$e = \frac{R_r}{R_r + R_L}.$$

Maximum power is delivered to the antenna when the impedance of the source is the complex conjugate of the antenna impedance. This is known as a conjugate match as shown in Figure 2.3(b) and is expressed by:

$$\begin{aligned} Z_S &= R_S + jX_S, \\ &= R_A - jX_A, \end{aligned}$$

where

$$\begin{aligned} R_S &= \text{Source resistance (ohms)}, \\ X_S &= \text{Source reactance (ohms)}. \end{aligned}$$

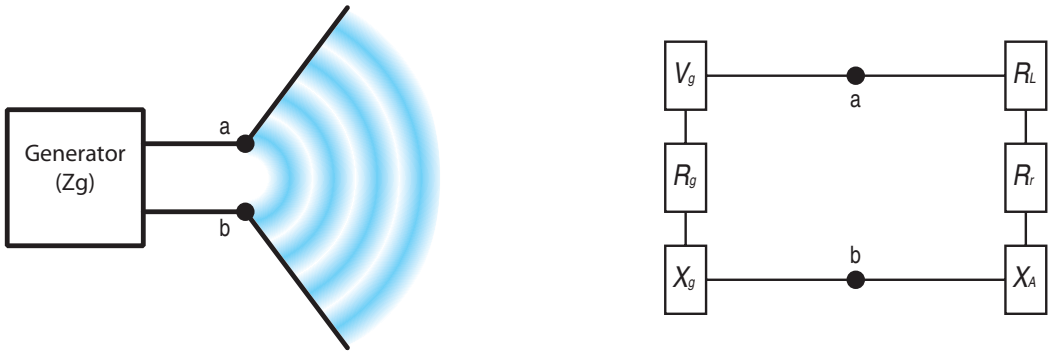

(a) Antenna in transmitting mode

(b) Antenna Thévenin equivalent circuit

Fig. 2.3: Antenna electrical characteristics. The antenna shown in Subfigure (a) is represented electronically by an equivalent circuit in Subfigure (b). The generator is on the left made up of the generator driving voltage V_g and impedance, R_g and X_g. The antenna element is on the right made up of the radiation resistance R_r, loss resistance R_L and antenna reactance X_A. Maximum power transfer between the generater and freespace is achieved when the source impedance is the complex conjugate of the antenna impedance.

In the case where the antenna is connected to the source by a transmission line, an electromagnetic wave travels from the source, through the different parts of the antenna system and out into free space. The antenna acts as a matching network that takes the power from the transmission line, and matches it to the free space impedance of 377 Ω. If the wave encounters differences in impedances as it propagates through the system, some fraction of the wave's energy will reflect back towards the source. The reflected energy forms a standing wave in the feed line. The ratio of maximum voltage to minimum voltage in the standing wave can be measured and is called the standing wave ratio.

The *bandwidth* of an antenna is the range of frequencies within which the performance of the antenna, with respect to some characteristic, conforms to a specified standard (IEEE Standard 1993). For broadband antennas it is convenient to express bandwidth as the ratio of the upper to lower frequencies of acceptable operation. While for narrow-band antennas the bandwidth is generally expressed as a percentage of the centre frequency.

Transmission and Reception

The *Friis transmission equation* (Friis 1946) describes how much power is directly coupled between two antennas while the *radar range equation* describes how much power is coupled between two antennas after reflection from an object. The Friss transmission equation for two impedance matched antennas is expressed by:

$$\frac{P_r}{P_t} = \Big(\frac{\lambda^2}{4\pi R^2}\Big) G_t G_r$$

relating the power delivered to the receiver P_r to the power generated at the transmitter P_t at a distance R.

The radar range equation makes use of a quantity known as *radar cross section*, denoted by σ, defined as the area intercepting that amount of power which, when scattered isotropically, produces at the receiver a density which is equal to that scattered by the actual target (IEEE Standard 1997). For polarisation matched antennas the radar range equation is expressed by:

$$\frac{P_r}{P_t} = \sigma \frac{G_t G_r}{4\pi} \Big[\frac{\lambda}{4\pi R_1 R_2}\Big]^2,$$

where R_1 is the distance of the target, with a radar cross section of σ, from the transmitting antenna and R_2 is the distance of the target from the receiving antenna.

2.2.2 Linear Antenna Array

An antenna array is two or more antennas coupled to a common source or load to produce a specific radiation pattern. The radiation pattern of a properly implemented antenna array is usually narrower with higher value of directivity than a single antenna element. Many applications benefit from antennas that concentrate their energy within a narrow beam, and the ability to vary the angle of that beam. These properties can be achieved by arranging multiple elements into an antenna array and exciting them appropriately.

The radiation pattern of the array is determined by the vector addition of the fields radiated by the individual elements. To achieve a directive pattern, the fields of each element must interfere constructively in the desired direction and destructively in all others. There are five properties used to control the radiation performance of an array (Balanis 1997):

1. the geometrical configuration of the array,
2. the relative displacement between the elements,
3. the excitation amplitude of the individual elements,
4. the excitation phase of the individual elements
5. the relative pattern of the individual elements.

Antenna array design is not the topic of this thesis. Therefore array theory is covered only briefly, focusing on linear phased arrays. Although mutual impedance and mutual coupling between antenna elements is beyond the scope of our phased array discussion, the concept is directly related to constrained lens port design and has thus been included.

Pattern Formulations

In general, the excitation of an array is defined by the voltage amplitude and phase at each element. Assuming identical elements in both construction and orientation, and neglecting mutual coupling, the far-field radiation pattern is the product of the isolated element pattern and the isotropic array factor (Pozar 1998). Therefore, the array radiation intensity, expressed in terms of the element radiation intensity U_e, is

$$U(\theta, \phi) \quad = \quad |\mathrm{AF}(\theta, \phi)|^2 U_e(\theta, \phi).$$

This is referred to as *pattern multiplication*. The isotropic array factor is the radiation pattern of the array where all antenna elements are replaced with theoretical isotropic elements.

The array factor for N equally spaced elements placed along the X-axis, as illustrated by Figure 2.4, is calculated by forming the vector sum of all elements in every direction θ.

The array factor is written as:

$$\begin{aligned} \text{AF} &= 1 + a_1 e^{j(kd\cos\theta+\beta)} + a_2 e^{j2(kd\cos\theta+\beta)} + \ldots + a_N e^{j(N-1)(kd\cos\theta+\beta)}, \\ &= \sum_{n=1}^{N} a_n e^{j(n-1)(kd\cos\theta+\beta)}, \\ &= \sum_{n=1}^{N} a_n e^{j(n-1)\psi}, \end{aligned}$$

where

$$\begin{aligned} \psi &= kd\cos\theta + \beta, \\ k &= \frac{2\pi}{\lambda}, \end{aligned}$$

and $a_1, \cdots, a_n$ is the magnitude of the excitation of each element, d is the spacing between elements, and β defines the slope of the phase delay between each adjacent element.

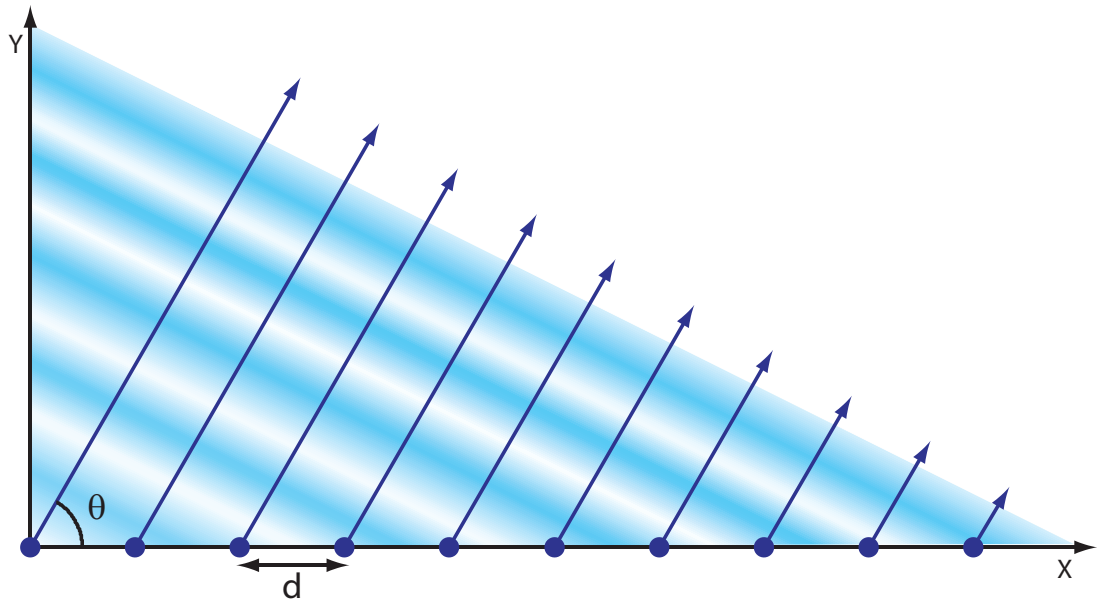

Figure 2.4: Antenna array beam-forming. The electromagnetic radiation generated by each antenna element is combined in the far-field. This field is described by the combination of the array factor and element beam pattern. The array factor is calculated, for all θ and ϕ, by forming the vector sum of all elements, blue dots spaced by distance d, in the far field.

A linear array of identically oriented and equally spaced radiating elements having equal current amplitudes, $a_1 \ldots a_n = 1$, and equal phase increments between excitation currents is referred to as a *uniform linear array* (IEEE Standard 1993). The array factor for a

uniform linear array can be further simplified to:

$$\mathrm{AF} = \left[\frac{\sin\left(\frac{N}{2}\psi\right)}{\sin\left(\frac{1}{2}\psi\right)}\right].$$

This simplified formula is used to calculate the angle of the array factor maximum, which includes the main beam, θ_0, and the grating lobes θ_G, and also the position of nulls and local maxima referred to as *side-lobes*. Furthermore, an approximate value for the 3 dB beam width and sidelobe level are easily obtained as depicted in Figure 2.5.

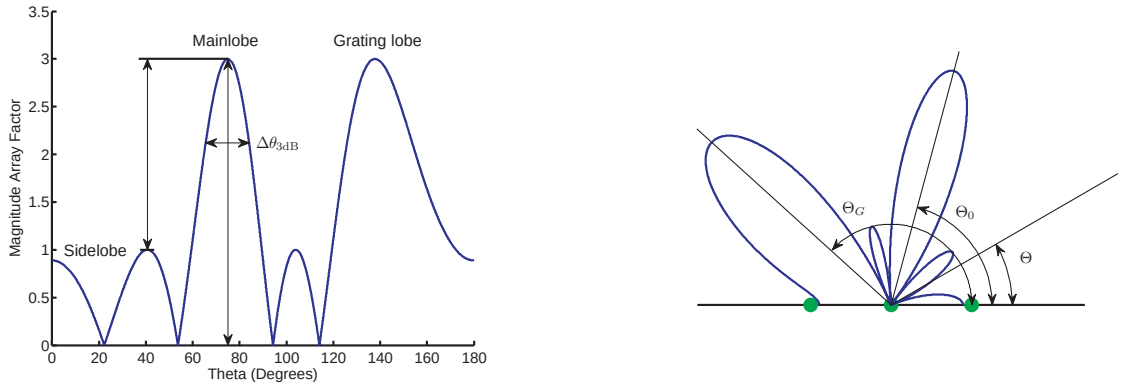

(a) Array Factor (b) Beam Pattern

Fig. 2.5: Array factor and beam properties. The beam pattern is described by a number of features, the main lobe, sidelobes, grating lobes, and the position of the beam maxima and nulls. The most important of these is the main-lobe described by the observation angle of θ_0 and the 3 dB beam width, $\Delta\theta_{3\mathrm{dB}}$. Other lobes that are often present are sidelobes, described by their magnitude relative to the mainlobe, and the grating lobes, located at θ_G. Subfigure (a) shows how the array factor varies with angle, while Subfigure (b) shows the beam pattern relative to the antenna elements represented by green dots.

The number of maxima present in the array factor depends on the spacing between elements, d. The position of the maximum and main beam is expressed by:

$$\begin{aligned}\theta_{\max} &= \cos^{-1}\left[\frac{\lambda}{2\pi d}(-\beta \pm 2m\pi)\right],\\ m &= 0, 1, 2...\end{aligned}$$

The maxima corresponding to $m = 1, 2\ldots$ are referred to as *grating lobes*. To ensure only one maximum is present, and therefore no grating lobes are present, the distance between

elements must be limited to:

$$d < \frac{\lambda}{1+|\cos(\theta_0)|}. \tag{2.2}$$

The direction of maximum radiation intensity, and $m = 0$, is referred to as the *observation angle*, θ_0. This is related to the relative phase delay β by:

$$\begin{aligned}\theta_0 &= \cos^{-1}\left(\frac{-\beta}{kd}\right),\\ &= \cos^{-1}\left(\frac{-\lambda\beta}{2\pi d}\right),\end{aligned}$$

or inversely

$$\beta = -\frac{2\pi d}{\lambda}\cos(\theta_0).$$

By varying β, the observation angle is swept through $-\pi$ to π as shown in Figure 2.6.

The radiation local maxima and nulls are calculated by examining when $\sin(\frac{N}{2}\psi)$ equals zero and 1. Therefore the position of the nulls is expressed by:

$$\begin{aligned}\theta_{\text{null}} &= \cos^{-1}\left[\frac{\lambda}{2\pi d}(-\beta \pm \frac{2n}{N}\pi)\right],\\ n &= 1, 2, 3...\\ n &\neq 0, N, 2N, 3N...,\end{aligned}$$

and the approximate position of the local maxima or side-lobes is expressed by:

$$\begin{aligned}\theta_{\text{s}} &\simeq \cos^{-1}\left[\frac{\lambda}{2\pi d}(-\beta \pm \frac{2s+1}{N}\pi)\right],\\ s &= 1, 2, 3...\end{aligned}$$

Approximations for beam width have been made (Balanis 1997):

$$\theta_{3\text{dB}} \simeq \frac{0.886}{\sin(\theta_0)}\frac{\lambda}{Nd}b.$$

The broadening factor b depends on the choice of the window and its sidelobe level. A *side-lobe* is a radiation lobe in any direction other than that of the main or grating lobes (IEEE Standard 1993). The maximum relative side-lobe level is the maximum relative directivity of the highest side lobe with respect to the maximum directivity of the antenna (IEEE Standard 1993). Low sidelobes, < -30 dB, are of interest for several reasons. Reducing sidelobes reduce radar and communications intercept probability, radar

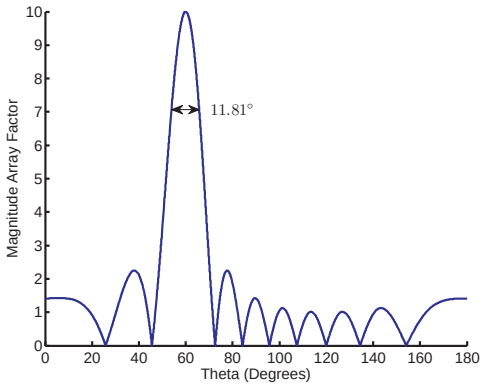

(a) 60 degree array factor

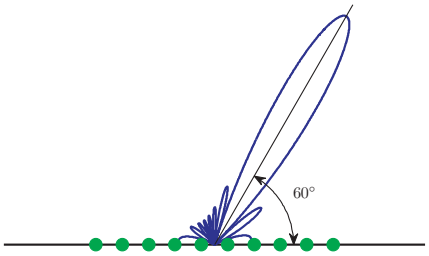

(b) 60 degree beam pattern

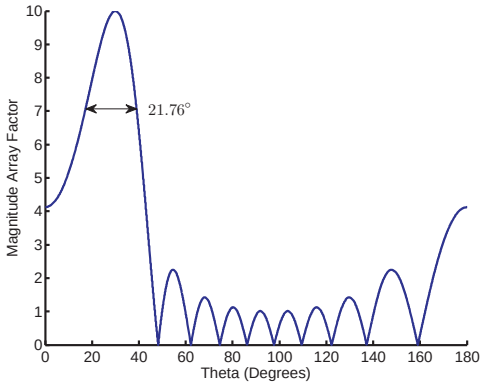

(c) 30 degree array factor

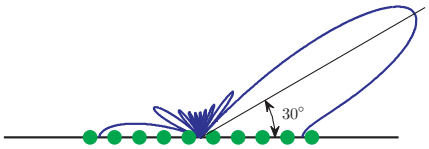

(d) 30 degree beam pattern

Fig. 2.6: Array scanning and beam width. The beam is scanned by varying the relative phase delay between elements, β. The width of the beam changes due to the reduction of the array's effective area as the beam is swept towards end-fire. Subfigures (a) and (c) show how the array factor varies with angle while Subfigures (b) and (d) show the beam pattern relative to the antenna elements represented by green dots.

clutter and jammer vulnerability, and spectrum congestion in satellite transmissions. To achieve a low sidelobe radiation pattern, the array excitation should be heavily tapered in amplitude.

The larger the sidelobe attenuation, the larger the broadening factor. Some examples of broadening factors for different windows are given as follows:

$$\begin{aligned}
\text{Rectangular}: &\quad b = 1, R = -13 \text{ dB} \\
\text{Hamming}: &\quad b = 2, R = -40 \text{ dB} \\
\text{Taylor-Kaiser}: &\quad b = \tfrac{6(R+12)}{155} \\
\text{Dolph-Chebyshev}: &\quad b = 1 + 0.636 \left[\tfrac{2}{R_a} \cosh\left(\sqrt{\text{acosh}^2(R_a) - \pi^2} \right) \right]^2
\end{aligned}$$

where R and R_a represent the sidelobe level in dB and absolute units, respectively.

The precise control of amplitude excitation along the length of the array is used to improve the sidelobe performance of the array as highlighted in Figure 2.7. The sidelobe levels of a uniform excitation is ≃-13 dB, Figures 2.7(a) and 2.7(b). By implementing a Hamming window excitation function, this will be reduced to ≃-40 dB at the expense of beam width and maximum directivity, Figures 2.7(c) and 2.7(d).

A grating lobe is a lobe, other than the main lobe, produced by an array antenna when the interelement spacing is sufficiently large to permit the in-phase addition of radiated fields in more than one direction (IEEE Standard 1993).

For half wavelength spacing of elements, a grating lobe appears at -90° for a beam scanned to +90°. When elements are spaced by one wavelength, grating lobes are present at ±90° for a beam at broadside as apparent in Figures 2.8(a) and 2.8(b). The significance of grating lobes is exacerbated for scanning arrays as any movement from broadside beam quickly moves the sidelobe away from the end-fire directions. Figures 2.8(c) and 2.8(d) show a grating lobe at 138° when the beam is scanned to 75° for an element spacing of one wavelength.

While Equation (2.2) ensures that only one maximum is present within the beam pattern, it does not prevent a large part of the grating lobe appearing at the edge of the radiation pattern. It is desirable to prevent any of the grating lobe appearing in the radiation pattern, as illustrated in Figure 2.8(b). By placing the pattern null adjacent to the grating lobe at ±90° the entire grating lobe is excluded. The array spacing reduction required to accomplish this is given by:

$$d \simeq \lambda \frac{N - \sqrt{1 + b^2}}{N(1 + \sin(\theta_0))}.$$

This is a general formula that applies to amplitude tapered distributions through the inclusion of the broadening factor b (Hansen 1997).

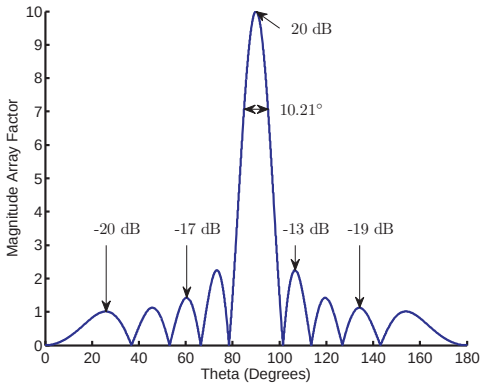

(a) Array factor of uniform excitation

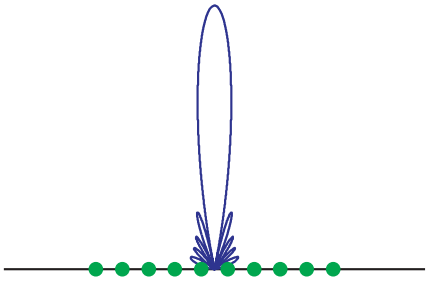

(b) Uniform excitation beam pattern

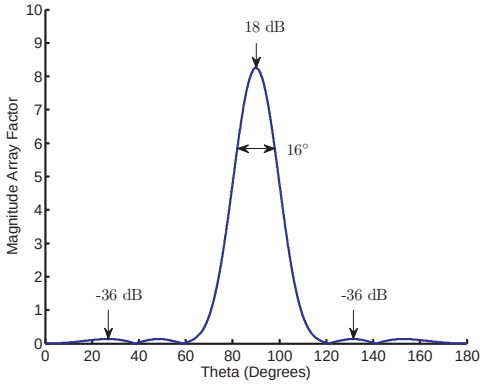

(c) Array factor of Hamming excitation

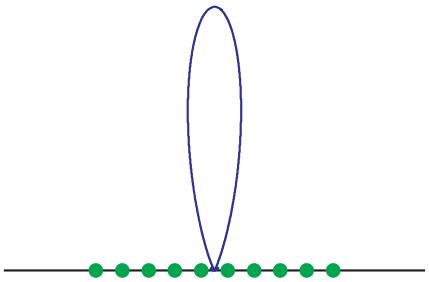

(d) Hamming excitation beam pattern

Fig. 2.7: Side-lobes and beam pattern. Careful choice of excitation taper will significantly reduce sidelobe levels. This figure compares a linear excitation with a Hamming excitation taper, highlighting the significant improvement in sidelobe level. The Hamming excitation taper has improved the sidelobe levels by 23 dB while increasing the width of the mainlobe by approximately 1.5 times. Subfigures (a) and (c) show how the array factor varies with angle while Subfigures (b) and (d) show the beam pattern relative to the antenna elements represented by green dots.

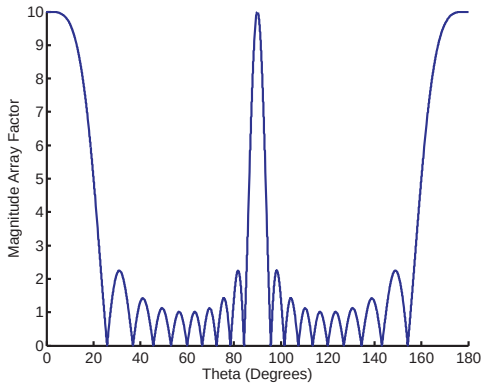

(a) Broadside grating lobe array factor

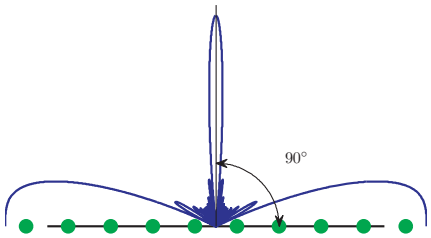

(b) Broadside grating lobe beam pattern

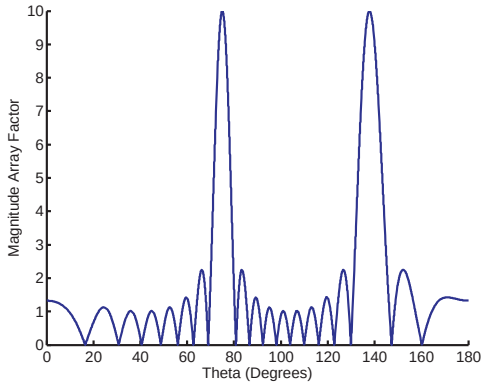

(c) Scanning grating lobe array factor

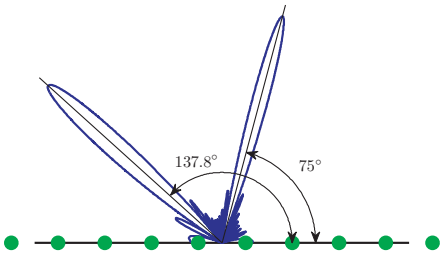

(d) Scanning grating lobe beam pattern

Fig. 2.8: Grating lobes and beam pattern. Increasing the spacing between elements beyond the limit defined by Equation (2.2) allows the in-phase addition of radiated fields at more than one angle. The repercussions of this are reduced width in the main-beam and additional lobes of equal magnitude to the main lobe. Subfigures (a) and (c) show the main lobe at 90° and grating lobes at 0° and 180°. Subfigures (b) and (d) show the main lobe at 75° and grating lobe at 137.8° for the same antenna element spacing. All figures are calculated for antenna element spacing of λ, represented by the green dots.

The bandwidth of an array is affected by many factors, including change of element input impedances with frequency, the existence of grating lobes, and change in element beamwidth. When an array is scanned with fixed units of phase shift, provided by phase shifters, there is also a bandwidth limitation as the position of the main beam will change with frequency. When an array is scanned with time delay, using variable path lengths, the beam position is independent of frequency to first order.

Mutual impedance and interaction between antennas

The interchange of energy between neighbouring antenna elements is known as *mutual coupling*. This energy is absorbed into the load connected to the antenna terminal or rescattered. Thus, the total contribution to the far-field pattern of a particular element in the array depends not only upon the excitation furnished by its own generator (the direct excitation) but upon the total parasitic excitation as well, which depends upon the couplings from and the excitation of the other generators (Allen and Diamond 1966). The strength of the mutual coupling depends primarily on the:

- radiation characteristics of each antenna,
- relative separation between elements,
- relative orientation of each element.

The input impedance of the antenna, in the presence of other elements, depends on the *self-impedance* and the *mutual-impedance* between the driven element and the other elements. The self-impedance is the input impedance of a radiating element of an array antenna with all other elements in the array open-circuited while the mutual-impedance is defined as the mutual impedance between any two terminal pairs in a multi-element array antenna is equal to the open-circuit voltage produced at the first terminal pair divided by the current supplied to the second when all other terminal pairs are open-circuited (IEEE Standard 1993).

The self impedance, Z_{11} and Z_{22}, and mutual impedance, Z_{12} and Z_{21}, are shown in Figure 2.9 for an array of two resonant monopoles. The variation in self and mutual impedance is shown for a range of element spacings and excitation frequencies. As expected, Figure 2.9(a) shows that the mutual impedance is reduced as element spacing is increased. Less obvious is that mutual impedance peaks at 5/3 of the resonant frequency of half wavelength spaced monopole antennas.

In order to maximise the radiated power for any one element in an array, the generator impedance should be a conjugate impedance match to the impedance seen at the element terminals while all elements are excited, rather than the impedance of the element when excited alone (Balanis 1997).

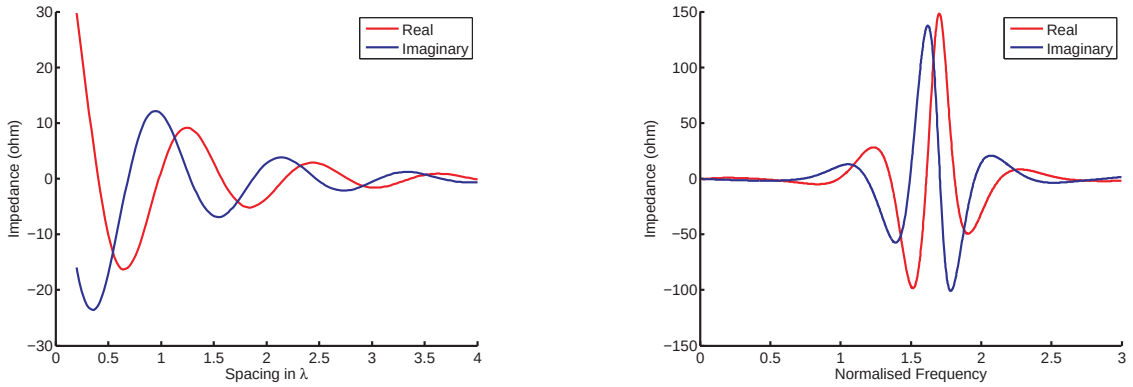

(a) Element spacing

(b) Frequency

Fig. 2.9: Monopole mutual impedance. The mutual coupling of two quarter wavelength monopoles is represented by the real and imaginary mutual impedance (Z_{12}, Z_{21}). Subfigure (a) shows the relationship between mutual impedance and element spacing. This figure show that interdependence of the antenna impedances increases as spacing is reduced. Subfigure (b) demonstrates the relationship with frequency normalised by the monopole self resonant frequency. While a resonant antenna produces a peak in mutual impedance near resonance, a broadband antenna displays a gradual increase in the magnitude of mutual impedance as frequency is reduced.

2.2.3 Summary

The radiation characteristics of an antenna array, directivity, beam width and sidelobes, are optimised by manipulating the phase and amplitude distribution between each element. The focus of this thesis is the design of multi-beam arrays, as such, the phase taper is the primary property controlling the direction of maximum array gain. Selection of amplitude taper is used to trade off beam width with sidelobe strength. Minimum beam width and maximum gain are achieved using a linear amplitude taper while reduced sidelobe strength requires a smooth taper that reduces in strength towards the edge of the array. The conflicting requirements force a compromise between high gain, narrow main beam, and power radiated within the sidelobes.

2.3 Beam-forming techniques

To present constrained lenses in context, alternative beam-forming techniques are now described. The discussion begins with techniques to produce a fixed single beam using series or corporate feeds. These basic feed structures, with the addition of phase shifters,

allow the concept of phased array scanning to be introduced. Finally, beam-forming networks are described, capable of producing multiple independent beams from a single linear array.

2.3.1 Single Fixed Beam Feeds

Fixed beam arrays are usually linear arrays. When the array elements are connected in series along a transmission line, the array is referred to as *series connected*. Similarly, when the elements are connected in parallel with a feed line or network, the array is referred to as *shunt connected*.

Series Feeds

The series feed network is most well known for its application in travelling wave slot antennas (Hansen 1997). The series feed consists of a single waveguide element connecting multiple antenna elements along its length. The resultant feed structure is only as long as the array, resulting in a very compact low-loss network. The regular spacing of the elements along the transmission line causes the system to resonate at the frequencies where the spacing becomes an integer multiple of half the wavelength.

Resonant arrays often have the end of the transmission line shorted to allow a standing wave to exist. The sum of the antenna reactances should equal zero while the sum of the antenna impedances is equal to the characteristic impedance of the line (Hansen 1997). As the the frequency varies, both the radiation pattern and input impedance of the array vary. The speed of the impedance variation is proportional to the number of elements. Therefore, resonant arrays are limited by narrow bandwidth and high input impedance.

A *travelling wave array*, like the resonant array, has radiating elements dispersed along a transmission line (Hansen 1997). Unlike the resonant array, the elements are not spaced by $n\lambda/2, n = 1, 2, 3\ldots$, and the transmission line is generally terminated by a matched load. As the energy propagates along the transmission line, each element radiates a small portion and the remaining energy is absorbed by the load. To achieve a linear excitation along the length of the array, elements near the feed must couple lightly to the transmission line, while elements near the load must couple heavily. Because of the non-resonant spacing, the main beam pattern will vary with frequency.

The beam squint that travelling wave arrays experience, as the frequency is varied, has been used to scan the main beam in a *frequency scanned array* (Hansen 1997). The

direction of the main beam is calculated by assuming that the radiating elements are spaced a physical distance d apart, and are connected by a feed with a length of s and guided wavelength of λ_g. The wavefront is defined by

$$\begin{aligned} kd\sin\theta_0 &= \frac{2\pi s}{\lambda_g} - 2\pi n, \\ n &= 1, 2, 3 \ldots \end{aligned}$$

The position of the main beam is calculated using:

$$\sin\theta_0 = \frac{s\lambda}{d\lambda_g} - \frac{n\lambda}{d}.$$

Clearly, larger s/λ, and correspondingly larger n, gives a faster change of beam angle with frequency. When the main beam becomes broadside or end-fire, the impedance of the array changes very quickly due to the in phase addition of element impedances (Hansen 1997). As a result, the field-of-view of this approach is limited to that between broadside and end-fire.

Corporate Feeds

A corporate feed structure connects multiple antenna elements by cascading power combiners/dividers. Such feeds commonly use binary branching, but sometimes the divider tree includes 3-way, or even 5-way dividers, depending upon the number of array elements. Figure 2.10 shows a simple binary parallel feed with phase shifters.

The critical component in the corporate feed is the power divider or combiner. While early corporate feed networks used waveguide dividers and hybrids (Riblet 1952, Hadge 1953), they can also be implemented very effectively in stripline or microstrip (Jones et al. 1958, Levy 1966, Young 1972). While many microstrip corporate feeds use the simple and compact split line power divider, other examples of power dividers or combiners include the broadband line coupler developed by Schiffman (1958); the popular Wilkinson divider incorporating resistive loads to improve the match (Wilkinson 1960); and the Lange coupler, which is a 90 degree hybrid coupler utilising interdigitated coupled lines (Lange 1969).

Distributed Arrays

The distributed array is another type of shunt feed network (Hansen 1961). A distributed array has each element connected to its own receiver/transmitter module. These systems

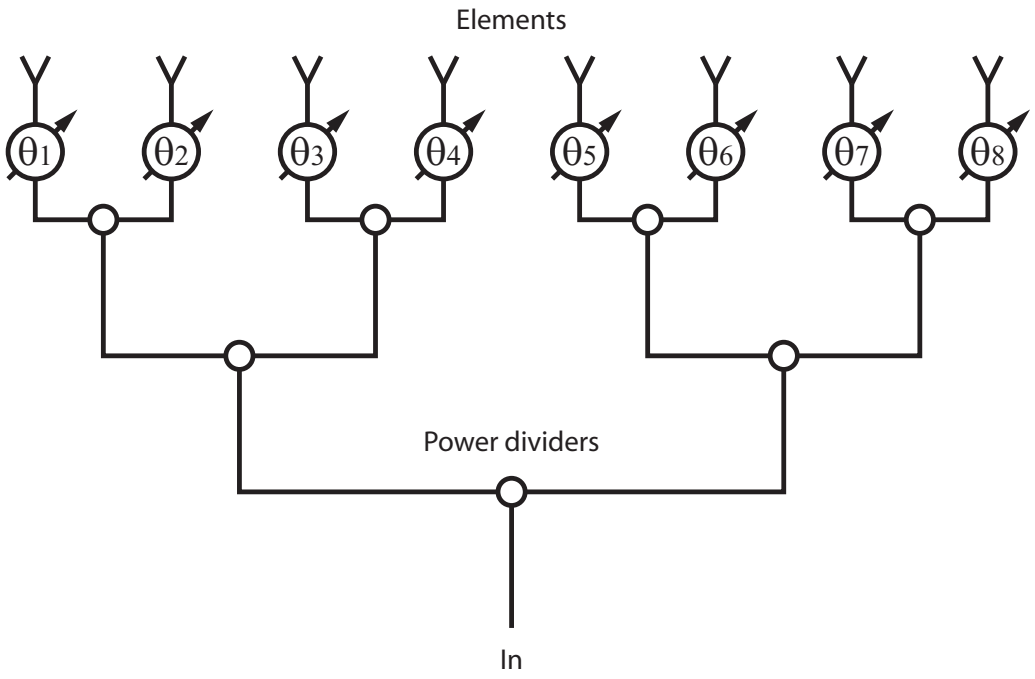

Figure 2.10: Binary power divider. Corporate feed networks are often used due to their simplicity. A corporate feed network connects multiple antenna elements by cascading power combiner/dividers. While this figure shows a corporate feed network using binary power splitters, triple and quadruple power splitters are also possible. This figure shows a corporate feed network feeding a phased array.

tend to have higher cost but have several advantages over simpler systems. Many low-power semiconductor sources are used instead of a single high-power source. Feed network loss is minimised, which increases the signal to noise ratio. Graceful degradation allows the system to continue to operate with small gain and sidelobe changes as each module fails. Therefore, mean time before failure is greatly increased (Hansen 1961).

2.3.2 Phased Array Scanning

A series feed or corporate feed is converted to a phased array feed by adding *phase shifters* in the feed line or connected to each element. These configurations are shown in Figure 2.11 and are referred to as *series phase shifters* and *parallel phase shifters*. Series phase shifters enjoy the advantage that all phase shifters have the same phase shift equal

to β. The disadvantage is that the first phaser must handle almost the entire power, and the phaser losses combine in series.

Parallel phase shifters experience less loss than series phase shifters because each phaser handles only $1/N$ of the transmitted power. The disadvantage is that each phaser must be capable of phase shift equal to the inter-element phase shift $\beta = kd\cos\theta_0$ multiplied by the number of the elements, N. At lower frequencies this is not a significant disadvantage as phase shifters capable of 2π phase shifting are relatively easy to produce (Hansen 1961, Balanis 1997). At higher frequencies or very broad bandwidths this requirement is much more difficult to achieve.

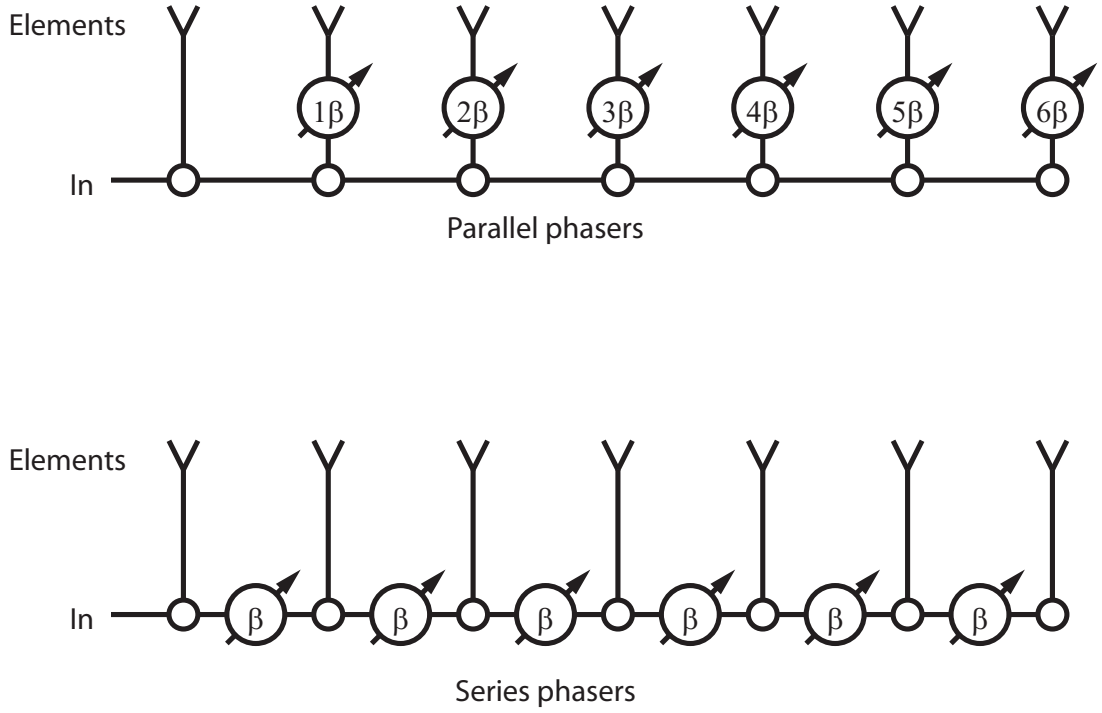

Figure 2.11: Phaser configurations. A phased array may be driven using parallel phase shifters, where phase shifters connected to each element, or series phase shifters where each phaser is placed in the feed between elements. Parallel phase shifters require large phase shifters because each successive phaser must be capable of $N\beta$ shift where N is the element number. Series phaser implementation uses identical phase shifters, however losses increase along the length of the array.

2.3.3 Beam-forming Networks

Multiple beam antennas allow a number of beams to be simultaneously transmitted and received from a single array aperture. Multiple-beam systems have applications in electronic countermeasures, satellite communications, multiple-target radars, and in adaptive nulling (Mayhan 1976). Multiple beamformers or beam-forming networks are either networks or quasi-optical lenses. In general, beam-forming matrices have beam crossover levels that are independent of frequency, while beamwidths and beam angles change with frequency. Lens beam formers have fixed beam angles, while beamwidths and hence crossover levels, change with frequency.

Power Divider Beamformer

The simplest beam-forming network is simply N fixed phase or time delay feeds connected to each element by a N-way power divider. The power divider causes a $1/N$ signal reduction making preamplifiers necessary to maintain the signal to noise ratio. This type of network is only practical for small numbers of beams and elements, however it has been used to drive as many as 91 elements and 16 beams (Metzen 1996).

Butler Matrices

A Butler matrix beam-forming network connects 2^n array elements, connected to an equal number of beam ports (Butler and Lowe 1961). It consists of alternate rows of hybrid junctions and fixed phase delays, shown in Figure 2.12(a) for a typical 8-element Butler network (Moody 1964). The Butler network is a simple network using components easily implemented in stripline or microstrip, however layout is difficult due to conductor crossovers.

The ideal Butler matrix is the analogue circuit equivalent of the fast Fourier transform (Butler and Lowe 1961, Shelton and Kelleher 1961), and an orthogonal system. An orthogonal system means that the network remains perfectly matched at all beam ports and no power is coupled between the beams. In practise this condition is only approximated by very narrow-band systems.

While the Butler matrix is capable of near-orthogonal performance for half-wave antenna spacing, and large element number, N, it can also be used to drive antenna elements with

other spacings. The beam position for generalised antenna spacing, d, is

$$\begin{aligned} \sin\theta_i &= \frac{i\lambda}{2Nd}, \\ i &= 1, 3, 5 \ldots (N-1). \end{aligned}$$

For half-wave element spacing the beams fill up visible space as demonstrated by Figure 2.12(b). The array is uniformly excited and the sidelobe level is -13.2 dB. When the element spacing is increased, the beamwidths become narrower and the beams move closer together. However, the crossover level remains -3.87 dB, as these effects cancel out.

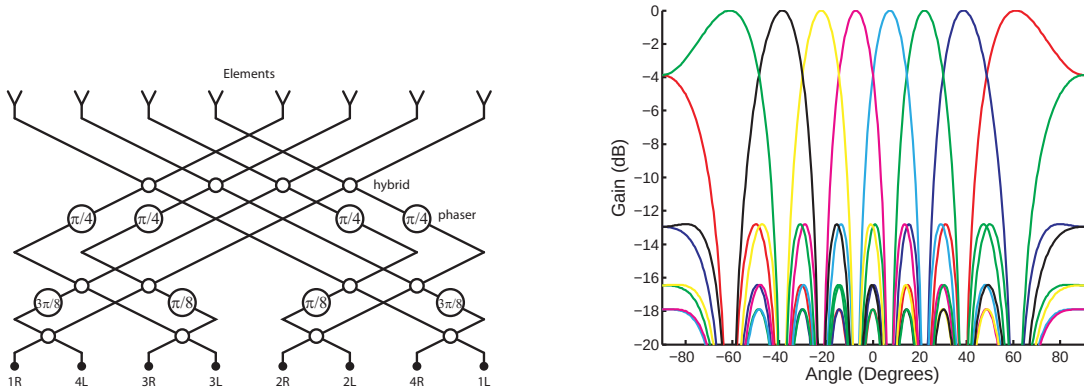

(a) Butler matrix circuit

(b) Orthogonal beams

Fig. 2.12: Butler matrix and beam pattern. The Butler matrix is a beam-forming network that uses phase delays and hybrid junctions to excite a number of simultaneous and independent beams. The number of beams and antenna elements is 2^N where N is the order of the matrix. The eight beams for the third order network shown in Subfigure (a) is shown in Subfigure (b). Each beam in plotted in a different colour.

Blass Matrices

The Blass matrix describes a set of array element transmission lines, which intersect a set of beam port lines, connected using directional coupler at each intersection (Blass 1960), as depicted in Figure 2.13(a). The Blass matrices consists of a number of travelling wave coupler arrays, where beam-forming is a result of the interaction these arrays. However these arrays are difficult to construct due to the sensitivity required of each coupler and the complexity of design due to the multiple interaction between couplers (Hansen 1997).

Nolen Matrices

The Nolen matrix (Nolen 1965) is a generalisation of both Blass and Butler matrices. The Nolen matrix is an analogue implementation of the general discrete Fourier transform algorithm and works for any number of elements. Owing to the high number of parts and the difficulties tuning the network, the Nolen beam-forming network is seldom used but is shown here for completeness, Figure 2.13(b).

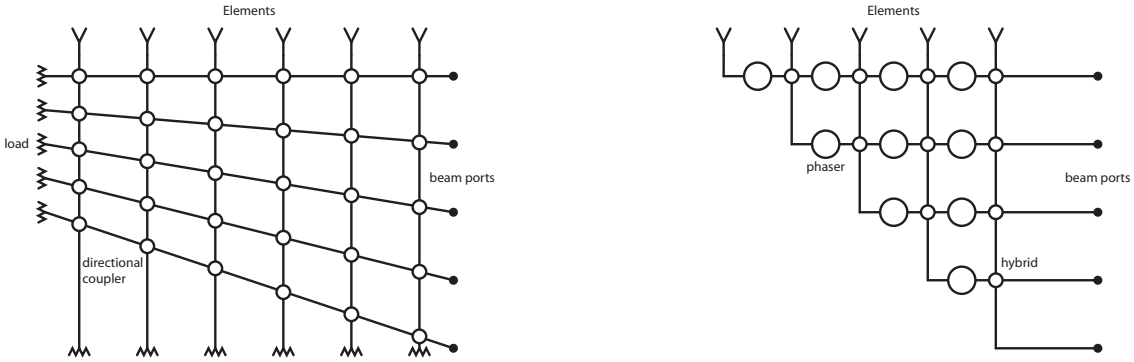

(a) Blass matrix circuit

(b) Nolen matrix circuit

Fig. 2.13: Blass and Nolen matrix circuits. The Blass and Nolen matrices shown in this figure are beam-forming networks similar to the Butler matrix. These Blass matrix shown in Subfigure (a) is difficult to implement due to the interactions between waves travelling between the large number of couplers. The Nolen matrix shown in Subfigure (b) is made impractical by the large number of components.

2.4 Constrained Lens Feeds

Constrained lenses fulfill the same function as dielectric lenses and reflector antennas. They collimate energy from a transmitting feed into a narrow beam, or focus a planar wave incident on a large aperture into a feed. In contrast to dielectric lenses, constrained lenses focus their energy via arrays of antennas connected by sections of transmission line. The combined effect of line length and antenna array geometry acts as a phase transformer or time delay, transforming a plane wave into a spherical or circular wave converging on a feed location.

The development of constrained lenses began with the single and dual focal point metal plate lenses of Kock (1946) and Ruze (1950). Figure 2.14(a) shows a single beam, metal plate lens. The parallel metal plates form both the antenna array and transmission lines connecting the antenna elements to the body of the lens. The transitions between the transmission lines and the body of the lens are referred to as antenna ports. The parallel plate section of the lens transforms the incoming planar wave into a circular wave. This wave propagates across the body of the lens, converging on a single feed location known as a beam port.

(a) Metal plate lens (b) Rotman lens

Fig. 2.14: Constrained lens examples. Subfigure (a) shows the layout of a metal plate lens. The lens is formed using the parallel metal plates on the right, to focus the incoming planar wave onto the single beam port on the left. Subfigure (b) shows a modern 37 GHz Rotman lens constructed using waveguide. The black material, each side of the lens, absorbs energy that would otherwise be reflected back into the lens from the sidewalls (Peterson and Rausch 1999b).

Constrained lenses provide low-cost, broadband, beam-steering networks. The trifocal Rotman lens and perfectly focused R2R lens (Hannan and Newman 1983, Hall and Vetterlein 1990) developments followed the metal lens. A wide variety of materials, transmission lines, and antenna types have been used; and the frequency of operation has been increased to near visible light (Sparks et al. 1998, Sparks et al. 1999).

Figure 2.14(b) shows a waveguide based Rotman lens designed to operate at 37 GHz (Peterson and Rausch 1999b). This lens uses waveguide to connect the antenna elements and the body of the lens. The beam ports and antenna ports are implemented using tapered waveguide sections that impedance match the waveguide to the body of the lens. Energy reflected from the sides of the lens can degrade the performance by increasing sidelobes and coupling between beam and antenna ports. The lens shown in Figure 2.14(b) uses Radiation Absorbing Material (RAM), shown in black, to absorb this energy, preventing it from being reflected back into the body of the lens.

2.4.1 Metal Lenses

Early forms of Ruze lenses (Ruze 1950) operate in a similar way to dielectric lenses (Hall and Vetterlein 1990) with the restriction that the rays within the lens must propagate parallel to the lens axis. This is represented by path $\overline{PQ}$ shown in red in Figure 2.15. The path in metal lens configuration is formed using parallel metal plates. The equations describing the ray path through the arbitrary path $\overline{PQ}$ and the path along the axis are solved for two focal points F_1 and F_2. The resultant solution is an elliptical inner contour, referred to as the lens contour. The shape of the lens contour is dependent on the lens thickness and the desired refractive index. The focal arc is a circle centred on the origin that passes through the two focal points.

Aberrations are a result of the path length variation of all paths from a point on the focal arc, through the lens, to the desired planar wavefront. The path length aberrations associated with a metal lens can be large and are highly dependent on the design of the lens. To combat abberations, refocusing of the lens is carried out by moving each point C on the focal arc radially, to find the position of minimum aberrations for each angular position θ on the lens contour. A portion of the refocused focal arc is shown by the dashed line in Figure 2.15.

The lenses take on different forms depending on how the equations describing the Ruze lens are applied. Figure 2.16 shows four types of Ruze lens designs. The constant thickness

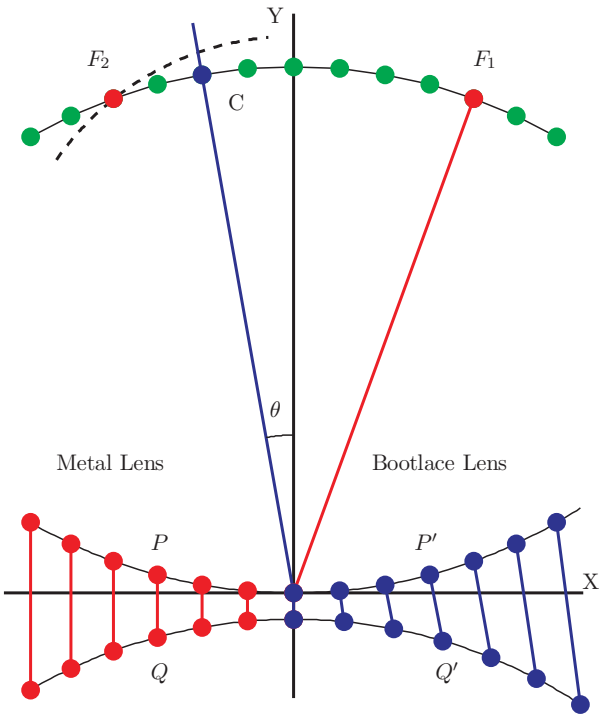

Figure 2.15: Geometry of a constrained lens. Both the metal lens and bootlace lens are solved for two focal points shown by the red dots at F_1 and F_2. The remaining beam ports, shown in green, are placed on a circular arc centred on the origin and joining these focal points. The errors associated with the remaining ports have been reduced by refocusing the focal arc shown by the dashed line. The metal lens on the left requires the paths connecting the antenna elements and antenna ports, the red lines labelled $\mathbf{P}$ and $\mathbf{Q}$, must be parallel to the lens axes. The bootlace lens on the right removes this restriction by allowing the antenna elements and ports to be connected using arbitrary lengths of transmission line as shown by the blue lines labelled $\mathbf{P}'$ and $\mathbf{Q}'$. This simple innovation adds the extra degree of freedom to the lens that later enabled the development of the Rotman lens.

lens shown in Figure 2.16(a) is small and compact but requires substantial refocusing. Figure 2.16(b) has a variable thickness but requires little refocusing. To reduce the size of this lens, Figure 2.16(c) has implemented zoning. Zoning is the process of varying the length of each path through the lens by a multiple of one wavelength. This means the lens is no longer a time delay beam-forming network. Instead it is a phase delay network that achieves perfect focus at multiples of the design frequency. Finally, Figure 2.16(d) shows a flat front lens requiring only a small amount of refocusing.

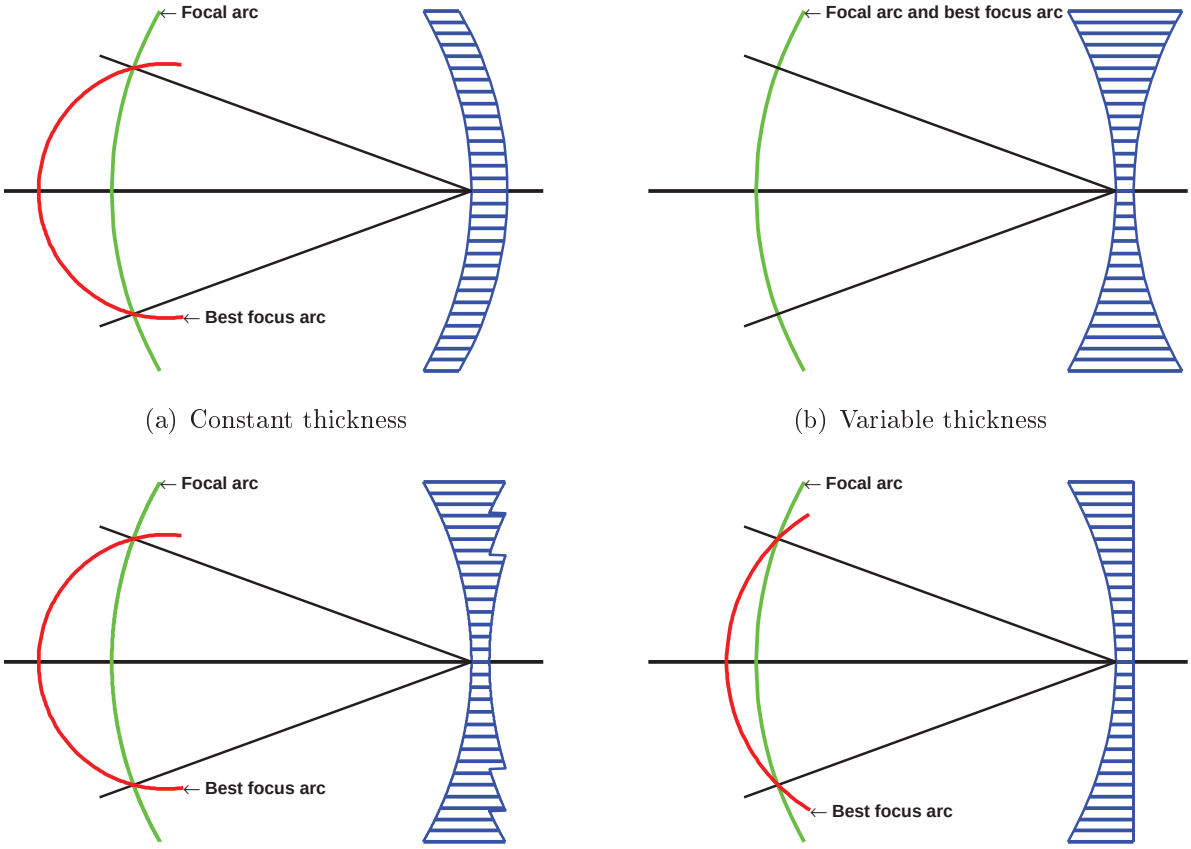

(a) Constant thickness

(b) Variable thickness

(c) Variable thickness with zoning

(d) Flat front

Fig. 2.16: Ruze lens configurations and refocusing characteristics. Four Ruze lens configurations based on the same lens requirement are shown. The choice of lens configuration has a significant effect on the refocused focal arc and lens size and weight (Ruze 1950). Subfigure (a) has a constant thickness but requires significant refocusing to achieve optimal performance. Subfigure (b) has a variable thickness and does not require refocusing but results in a very heavy lens. This weight is reduced using zoning in Subfigure (c) by stepping the lens by multiples of a wavelength. Subfigure (d) uses a flat front face and requires limited refocusing.

2.4.2 The Bootlace Lens

Until the bootlace lens was reported by Gent (1957), constrained lenses were treated merely as a convenient refractive medium. The bootlace lens changed this perception by considering constrained lenses as arrays of antennas connected by lengths of transmission line. The first antenna array forms the input contour and the second is referred to as the lens contour. The lens is then driven by individual antennas placed along the focal arc.

The bootlace aerial demonstrated that constrained lenses could be implemented using a wide variety of transmission line types connecting several types of radiators. The use of non-dispersive transmission lines, coax or parallel wire cable for example, make very broadband lens systems practical. Microstrip or stripline implementations, combined with a high dielectric substrate, allow very compact constrained lenses to be built (Maybell 1981).

The bootlace lens is similar to the Ruze lens except that the path $\overline{P'Q'}$ in Figure 2.15 is no longer required to be parallel to the axis. Instead $\overline{P'Q'}$ can be specified independently of the input and output element positions. Gent (1957) demonstrated this using a simple antenna array consisting of two ground planes, separating folded dipole radiators, connected by parallel wire cables. By decreasing the length of the connecting transmission lines towards the outside of the lens, the wavefront is slowed in the middle of the lens relative to the outside, focusing the wave onto a single point.

The three degrees of freedom available in the metal lens are supplemented by a fourth in the bootlace lens (Gent 1957). The four degrees of freedom are:

1. the shape of the input contour or antenna array;
2. the shape of the output contour or lens contour;
3. the length of the transmission line connecting corresponding antenna elements and antenna ports;
4. the relative positions of the antenna elements and antenna ports on the antenna array and lens contour respectively.

Gent et al. (1956) considered several bootlace lens based antenna designs that describe most practical constrained lens antennas. Examples of these, shown in Figure 2.17, are:

1. the *Parasitic Array Mirror* or reflect-array which has only one surface, short-circuiting the transmission lines connected to each element;

2. the *Variable Line-Length Scanning Lens* has rotary phase shifters between the lens faces to achieve wide angle scanning while the lens covers a narrow sector;

3. the *Stepped Parasitic Array Lens* implements zoning by reducing the transmission line lengths by increments of a wavelength. This reduces the total line length required at the expense of bandwidth;

4. the *Attenuation Control* has attenuators inserted in the transmission lines to control the aperture amplitude distribution. This is used to reduce sidelobes or implement beam shaping;

5. the *Active Aerial* has high-power transmitting amplifiers inserted in each of the transmission lines. This achieves high output power without the need for a single very high power amplifier;

6. the *Polarisation Changing Aerial* implement differing polarisations on the front and back faces of the lens.

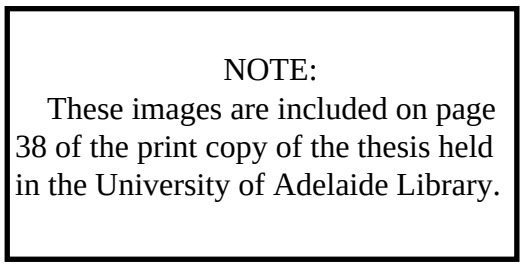

(a) Parasitic Array Mirror

(b) Variable line length scanning lens

(c) Stepped parasitic array lens

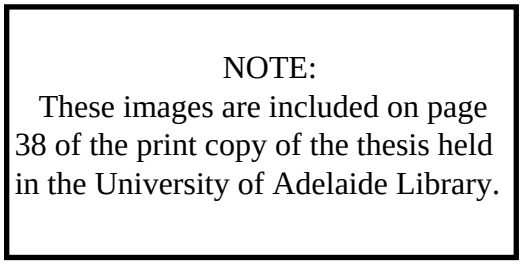

(d) Attenuation control

(e) Active aerial

(f) Polarisation changing aerial

Fig. 2.17: Fundamental bootlace lens types. These sub figures show the fundamental bootlace lens types described by Gent et al. (1956). All practical bootlace lenses can be thought of as a combination of these six configurations. Subfigure (a) is the parasitic array mirror and operates in the same way a parabolic reflector does. Subfigure (b) uses variable line lengths or phase shifters to scan the beam. Subfigure (c) steps the line lengths by multiples of λ_g to reduce the length of the larger delay lines. Subfigure (d) uses attenuators to control the excitation taper of the antenna array. Subfigure (e) achieves large output power by combining each antenna element with a small amplifier. Finally, Subfigure (f) uses polarised antenna elements to change the polarisation of the incident wave.

2.4.3 Circular Apertures

In contrast to the lens topologies described so far, the R2R and RKR lens make use of a uniformly spaced circular antenna array instead of a linear antenna array. The R2R geometry is unique because it is perfectly focused for all beam angles, however it is limited by a maximum field-of-view of 180 degrees. The RKR lens is able to scan through 360 degrees but has no perfect focal points.

R2R Lens

The R2R lens concept originated during wartime work on microwave radar (DeVore and Iams 1948, Myers 1947) and the original application used line-source antennas (Clapp 1984). The R2R lens is named because the outer radius is twice that of the inner radius and the angular spacing of the lens ports is twice that of the antenna elements. This results in equal spacing of both lens ports and antenna elements. The elements of the lens are connected to array elements using equal line lengths. An example of a R2R

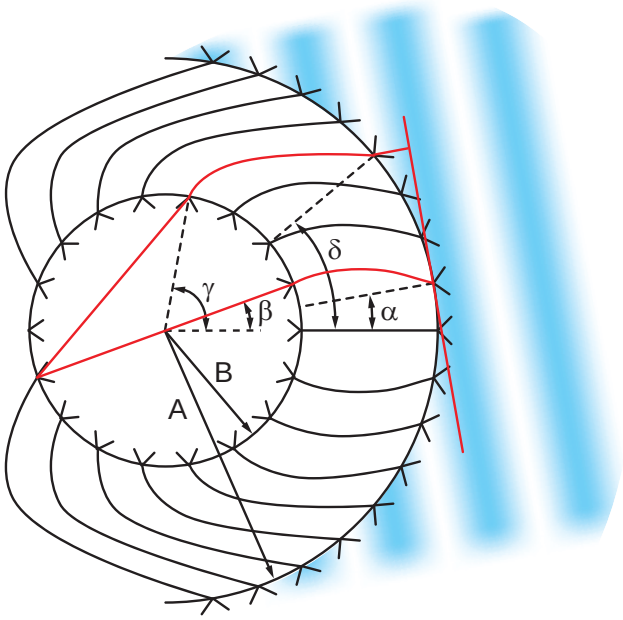

Figure 2.18: R2R lens topology. The R2R lens topology consists of an circular lens contour with radius B and a circular antenna contour of radius A. The positions of the lens ports are defined by β and γ while the position of the antenna elements are defined by α and δ. By setting the radius A twice that of B, perfect beam-forming is possible at every beam port.

lens layout capable of scanning up to 180 degrees is shown in Figure 2.18 (Boyns et al. 1968, Provencher 1970).

For a circular array to generate a plane wave directed at an angle α, the elements must have a path length difference of

$$d = A(1 - \cos(\delta - \alpha)),$$

where δ is the angular position of the antenna element and A is the outer radius. A feed positioned at $(\beta + 180°)$ will be a length R from each point on the lens given by

$$R = 2B\cos(\frac{\gamma - \beta}{2}),$$

where γ is the angular position of the antenna element and B is the radius of the lens. The path length equality condition is

$$R + d = 2B.$$

This can be written as

$$2B(1 - \cos(\gamma/2 - \beta/2)) = A(1 - \cos(\delta - \alpha)). \quad (2.3)$$

It is obvious that for $A = 2B$, $\gamma = 2\delta$ and $\beta = 2\alpha$, the above condition is always satisfied.

The R2R lens is particularly interesting because Equation (2.3) is satisfied for all β making the lens capable of aberration free scanning.

RKR Lens

The R2R lens design is limited by its maximum field-of-view of 180° and its ability to feed only half of a circular antenna array. The RKR lens utilises the entire circular antenna array and enjoys a field-of-view of 360° (Provencher 1970, Jodelson et al. 1979b, Jodelson et al. 1979a, Clapp 1984). This is achieved by placing the antenna elements at the same angular position as the lens ports. The antenna ports and beam ports are connected using equal length transmission lines containing a circulator as shown in Figure 2.19.

The equal angular spacing of antenna elements and lens ports means that Equation (2.3) becomes

$$2B(1 - \cos(\gamma/2 - \beta/2)) = A(1 - \cos(\gamma - \alpha)).$$

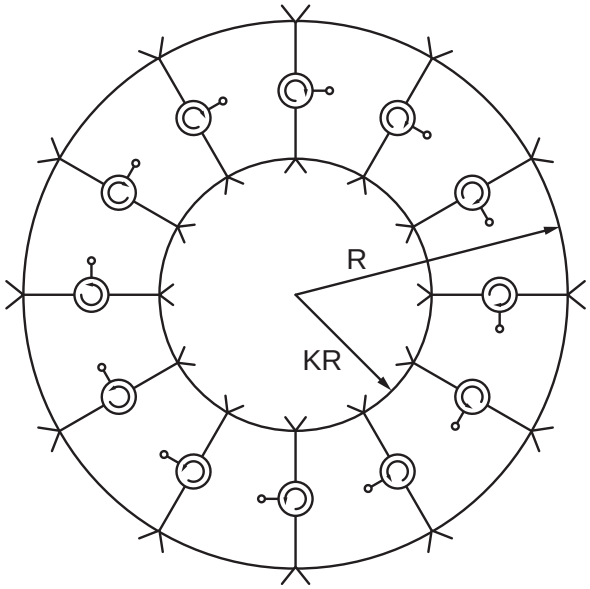

Figure 2.19: RKR lens topology. The topology of the RKR lens places antenna elements at the same angular position as the beam ports and antenna ports. The beam ports are fed by a circulator. The ratio of the inner to outer radius, K, is optimised to minimise the phase errors of the wavefront. The RKR lens does not have any perfect focal points but is able to produce beams across a 360° field-of-view.

This equation does not have a solution for all α and γ. Aberrations can be minimised by the careful selection of A and B. Figure 2.20 plots the path length error from:

$$\triangle l/A \;\; = \;\; 2K(1-\cos(\gamma/2-\beta/2))-(1-\cos(\gamma-\alpha)),$$

for five values of K where $B = KA$. The graph shows that values between 1.7 and 1.9 result in acceptable path length errors. The resultant lens is then approximately twice the size of the antenna array. To be practical the lens size must be reduced using dielectric material if it is to fit inside the array. Lenses have been reported which are capable of -20 dB sidelobes with 10° beams covering 360° at 11 GHz (Archer 1984).

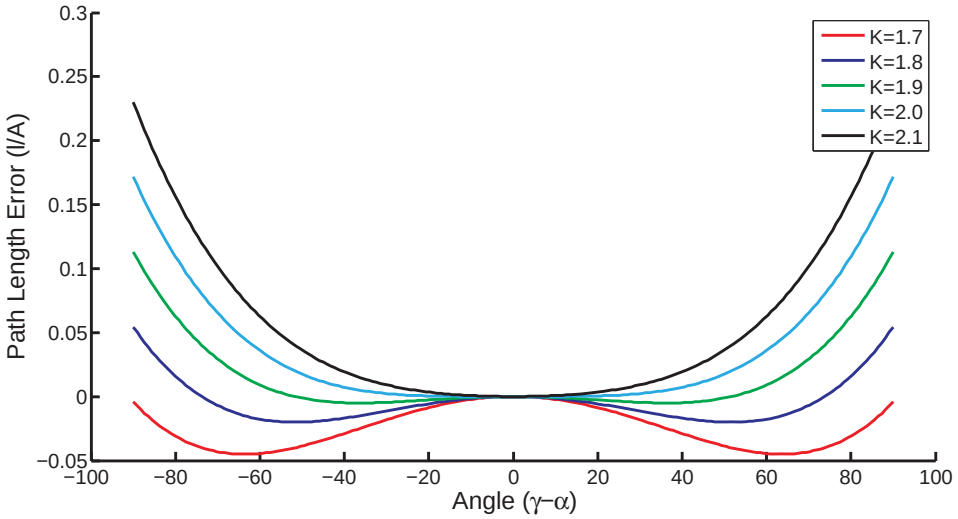

Figure 2.20: RKR path length aberrations. The RKR lens optimises the ratio of the inner lens contour and the outer antenna contour to minimise the magnitude of the path length aberrations. This figure shows the path length error versus aperture angle for a RKR lens for $K = B/A = 1.7, 1.8, 1.9, 2.0, 2.1$. Setting $K \approx 1.9$ produces a lens with very small aberrations for $|\gamma - \alpha|$ <50°.

2.4.4 Rotman Lens

The Rotman lens (Rotman and Turner 1963) is one of the most useful linear array feed networks due to its excellent aberration characteristics and frequency-invariant beam pointing. The Rotman lens achieves path length errors an order of magnitude smaller than that of dual focal point lenses (Smith 1982). The excellent aberration characteristics are a product of an additional focal point made possible by the extra degrees of freedom offered by the bootlace lens. This improvement in performance satisfies the low phase error requirements of wide apertures forming narrow beams. For this reason the Rotman lens has become the accepted standard when driving linear antenna arrays.

NOTE:
This figure is included on page 43
of the print copy of the thesis held in
the University of Adelaide Library.

Figure 2.21: First Rotman lens. Designed by Rotman and Turner (1963), the first Rotman lens consisted of 37 antenna ports, connected to a linear array, and 3 beam ports at 0°, 15°, and 30°. The Rotman lens uses the extra degree of freedom, available in the bootlace lens, to realise a third perfect focal point on the axis of the lens. Adapted Rotman and Turner (1963).

The first Rotman lens is shown in Figure 2.21. It was constructed using reflector backed E-plane probes mounted between two parallel plates, excited by H-plane sectorial horns (Rotman and Turner 1963). The width of the beam ports was varied to approximate a cosine illumination excitation taper in an attempt to obtain a sidelobe level of -23 dB. However, measurement showed sidelobe levels of only -18 dB. This lens demonstrated

the feasibility of the Rotman lens and the low aberration performance revolutionised constrained lens design.

The Rotman lens is designed using a simple set of equations that relate the position of each element of a linear antenna array, to the position of an antenna port, based on the positions of three focal points. One of the focal points is situated on the axis of the lens and the other two are placed symmetrically ether side. These equations are described in detail in Section 4.2.1. The design equations do not define the shape of the focal arc connecting the three focal points or the sidewall connecting the antenna port arc to the focal arc. The optimal choice of focal point position and focal arc choice has generated significant discussion in the literature. This discussion is presented in Chapter 4 with a summary of Rotman lens construction techniques and examples found in the literature.

2.5 Chapter Summary

Rotman lenses have proved a popular multiple beam-forming technology, due to their simplicity and performance. They have been overtaken by developments in digital signal processing and the speed of analogue to digital converters. The result is that many of these applications now use digital beam-forming techniques instead. The applications that remain, operate at millimetre wavelengths, have bandwidths of many gigahertz, or must drive so many beams that digital techniques are not practical or affordable.

This thesis examines the construction of monolithic constrained lenses using microstrip or stripline. These manufacturing techniques are mature, inexpensive and support the construction of lenses at millimetre wavelengths and into the terahertz band.

While understanding the Rotman lens design equations need only a basic understanding of geometry, to manifest these simple concepts into a functional beam-forming network requires a sound understanding of transmission line theory and design. To this end, the following chapter gives an overview of transmission lines, network parameters, and impedance matching circuits.